

Measuring Self-Supervised Representation Quality for Downstream Classification using Discriminative Features

Neha Kalibhat^{*1}, Kanika Narang², Hamed Firooz², Maziar Sanjabi², Soheil Feizi¹

¹Department of Computer Science, University of Maryland - College Park

²Meta AI

Abstract

Self-supervised learning has shown impressive results in downstream classification tasks. However, there is limited work in understanding their failure modes and interpreting their learned representations. In this paper, we study the representation space of state-of-the-art self-supervised models including SimCLR, SwaV, MoCo, BYOL, DINO, SimSiam, VICReg and Barlow Twins. Without the use of class label information, we discover discriminative features that correspond to unique physical attributes in images, present mostly in correctly-classified representations. Using these features, we can compress the representation space by up to 40% without significantly affecting linear classification performance. We then propose Self-Supervised Representation Quality Score (or Q-Score), a model-agnostic, unsupervised score that can reliably predict if a given sample is likely to be mis-classified during linear evaluation, achieving AUPRC of 91.45 on ImageNet-100 and 78.78 on ImageNet-1K. Q-Score can also be used as a regularization term on any pre-trained self-supervised model to remedy low-quality representations. Fine-tuning with Q-Score regularization can boost the linear classification performance of state-of-the-art self-supervised models by up to 5.8% on ImageNet-100 and 3.7% on ImageNet-1K compared to their baselines. Finally, using gradient heatmaps and Salient ImageNet masks, we define a metric to quantify the interpretability of each representation. We show that discriminative features are strongly correlated to core attributes and enhancing these features through Q-score regularization makes representations more interpretable across all self-supervised models.

1. Introduction

Self-supervised models [13, 11, 14, 26, 15, 8, 31, 12, 3, 49] learn to extract useful representations from data without relying on human supervision, and perform comparably to supervised models in downstream classification tasks. Pre-training these models, however, is extremely time-consuming and resource-intensive. It is therefore crucial that the learned representations are of high quality such that they are explainable and generalizable. However, in practice, these representations are often quite noisy and uninterpretable, causing difficulties in understanding and debugging their failure modes [30, 29, 23].

In this paper, our goal is to study the representation space of pre-trained self-supervised models such as SimCLR [13], SwaV [11], MoCo [14], BYOL [26], SimSiam [15], DINO [12], VICReg [3] and Barlow Twins [49] and discover their informative features in an unsupervised manner. We observe that representations are mostly sparse, containing a small number of *highly activating features* (Figure 2). These features can strongly activate a small, moderate or large number of samples in the population. We refer to the moderate category of features as *discriminative features*.

We observe some intriguing properties of discriminative features: (i) Although discovered without any class label information, they can be strongly correlated to a particular class or group of classes (See Figure 1); (ii) They highlight useful/informative attributes in the activating samples which are often related to the ground truth of those samples; (iii) There are more such features in correctly classified representations than mis-classified representations (as shown in Figure 4) and finally, iv) Representations can be compressed by up to 40% using discriminative features without significantly affecting linear evaluation performance.

Building on these observations, we propose a model-agnostic, unsupervised, sample-wise **Self-Supervised Representation Quality Score (Q-Score)**. A high Q-Score for a sample implies that its representation contains highly activating discriminative coordinates which is a favorable

^{*}Correspondence to nehamk@umd.edu

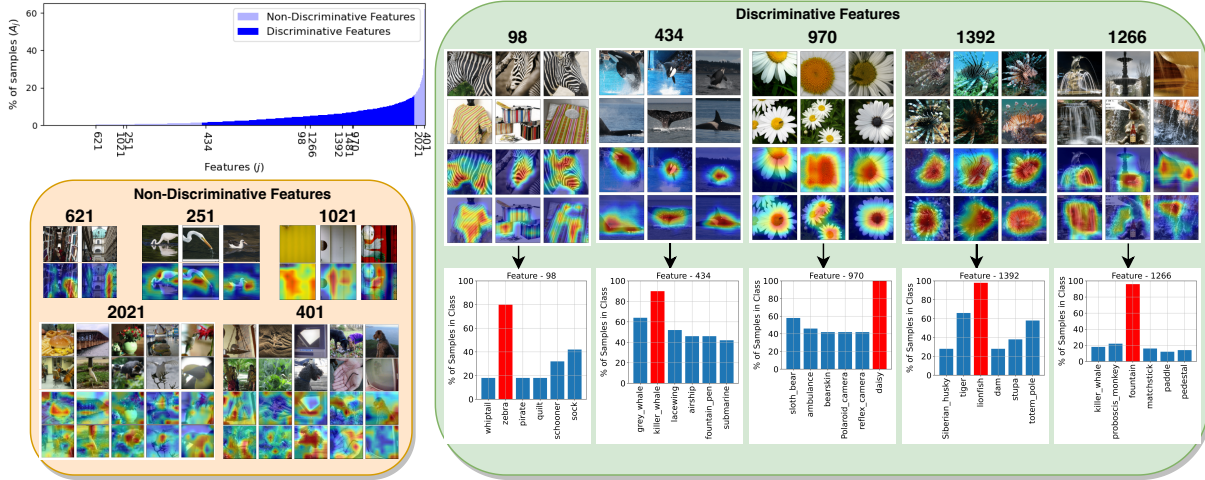


Figure 1. **Discriminative Features in Self-Supervised Models:** We plot the percentage of highly activating samples for each feature in the SimCLR [13] (ResNet-50 [27]) representation space. The features that show very low or very high percentage activations are *non-discriminative* as they likely correspond to very uncommon (lower tail) or very general attributes (upper tail). The features that activate a moderate number of samples (middle portion) are called *discriminative features*. As shown in the gradient heatmaps, these features encode important physical attributes shared among specific classes. These features play a key role in assessing the quality of self-supervised representations for downstream linear classification tasks.

representation property. We empirically observe that Q-Score can be used as a zero-shot predictor in distinguishing between correct and incorrect classifications for any self-supervised model achieving AUPRC of 91.45 on ImageNet-100 and 78.78 AUPRC on ImageNet-1K.

We next apply Q-Score as a regularizer and fine-tune pre-trained self-supervised models to improve low-quality representations. Across all baselines, Q-Score regularization improves the linear classification accuracy. On BYOL, we observe the highest improvement of 5.8% on ImageNet-100 and 3.7% on ImageNet-1K. The representations, after regularization, show increased activations for discriminative features (Figure 4) due to which several previously mis-classified samples get correctly classified with higher confidence.

Finally, we define a metric for quantifying representation interpretability by computing mean Intersection over Union (mIoU) with Salient ImageNet [40] masks used as ground truth. We show that, across all baselines, the discriminative features of self-supervised representations are strongly correlated to *core* features of Salient ImageNet. We can therefore interpret these features better by potentially correlating their meanings with the worker annotations provided for core features in Salient ImageNet. We also observe that mis-classified representations in our baselines show relatively lower IoU scores with core features compared to correct classifications. However, after Q-score regularization, we observe that the interpretability of mis-classified representations also improves via discriminative features.

We summarize our contributions as follows:

- We study the representation space of self-supervised models and discover *discriminative features* which often have unique physical meaning and mostly exist in correctly-classified representations. Although these features are discovered without any label information, they do show strong correlation to class labels.
- We introduce Self-Supervised Representation Quality Score (Q-Score), a model-agnostic, unsupervised score, to measure the quality of each learned representation. We empirically observe that the higher the Q-Score, the more likely that the sample will be correctly classified, achieving an AUPRC of up to 91.45 on ImageNet-100 and 78.78 on ImageNet-1K.
- We apply Q-Score as a light-weight regularizer to the self-supervised loss and show that, by improving the quality of low-score samples, we can improve downstream classification accuracy by up to 5.8% on ImageNet-100 and 3.7% on ImageNet-1K. We also define an interpretability metric to show that using the Q-Score regularization produces more explainable representations.

2. Related Work

Unsupervised methods for classification has been a long-standing area of research, generally involving the use of clustering techniques [5, 20, 47, 4, 9, 10, 28]. Self-supervised learning, is a recent approach to learn without human supervision by training models to prepare their own labels for each example [5, 20, 45, 19] usually with the help

of a contrastive loss. Contrastive learning [1, 43, 2] usually uses a temperature-controlled cross-entropy loss between positive pairs of *similar* samples and negative pairs of *dissimilar* samples. Positive pairs are usually considered as multiple transformations (views) [41] of a given sample using stochastic data augmentation. Through this approach, several state-of-the-art self-supervised techniques [13, 11, 15, 26, 14, 31] have produced representations that show linear classification accuracy comparable to that of supervised approaches.

Understanding these learned representations is relatively less explored. [30], observes that self-supervised representations collapse to a lower dimensional space instead of the entire embedding space. Other methods [44, 46], propose to separate the representation space into variant and invariant information so that augmentations are not task-specific. [25] observes representations across layers of the encoder and compare it to supervised setups. Clustering-based or prototypical-based methods have also been proposed where the representation space is collapsed into a low-rank space [21, 32]. [6] uses an RCDM model to understand representation invariance to augmentations. [24] proposes a score based on the rank of all post-projector embeddings that can be used to judge and compare various self-supervised models.

In this work, we focus more on studying representations across correct and incorrect classifications in downstream classification tasks and understanding their properties (without using any labels). We investigate the connection between these unsupervised properties in the representation space and mis-classifications. Unlike [24] which requires computing rank over the entire dataset, our analysis leads to the development of an unsupervised *sample-wise* quality score which can be used as a regularizer and effectively improve downstream classification performance.

3. Understanding Representations and their Failure Modes

Let us consider a pre-trained self-supervised model with a ResNet [27] backbone encoder $f(\cdot)$. Given an input sample, $\mathbf{x}_i \in \mathbb{R}^n$ its representation is denoted by, $f(\mathbf{x}_i) = \mathbf{h}_i \in \mathbb{R}^r$, where r is the size of the representation space. Our goal is to study this representation space and identify the properties which are essential for better downstream performance.

In the top panel of Figure 2, we visualize the representations of SimCLR pre-trained on ImageNet-1K [38]. Each row denotes the representation vector (\mathbf{h}_i) of a random sample drawn from the the ImageNet-1K validation set. There are 2048 columns corresponding to the representation size of a ResNet-50 [27] encoder. In all our analysis, we perform L2 normalization over every representation vector \mathbf{h} to ensure fair comparison of features.

First, we study some visual properties of these repre-

sentations. We observe that each representation is *nearly* sparse, i.e., most feature values are close to zero [30]. However, there exists a select few features that are strongly deviated from the remaining features in any given representation. We verify this observation in the second panel of Figure 3 where, we plot the distribution of all the SimCLR features of the same samples as the top panel, as well that of other self-supervised models including, DINO [12], SwaV [11], MoCo [14], VICReg [3] and Barlow Twins [49]. In each distribution, a very large number of features have a magnitude of 0 or very close to 0. In the zoomed version of the same plot, we can see a relatively small number of features that show strong activations. For any given representation $\mathbf{h}_i \in \mathbb{R}^r$, we formally define the **set of highly activating features** (L_i) as $L_i := \{j : h_{ij} > \mu_i + \epsilon\sigma_i\}$, where μ_i and σ_i denote the mean and standard deviation of \mathbf{h}_i respectively and ϵ is a hyperparameter that is empirically selected. We use $\epsilon = 4$ in our experiments. For every feature j , the percentage of highly activating samples is denoted by, $A_j = \frac{100}{N} \sum_{i=1}^N \mathbb{1}_{j \in L_i}$ where N is the size of the population. In Figure 1 top panel, we plot A_j for all features j in the SimCLR representation space of the ImageNet-1K validation set. The x-axis is ordered in ascending order of A_j .

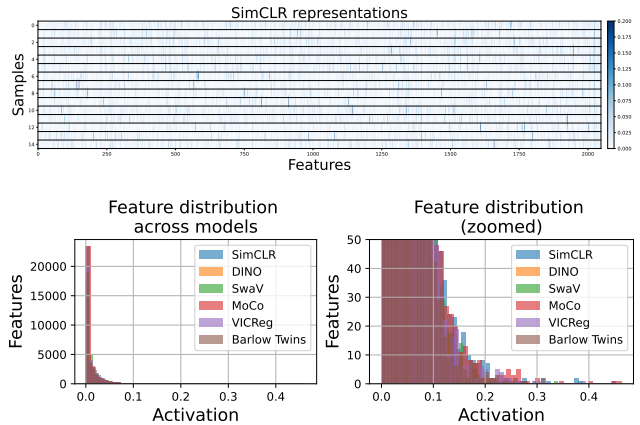


Figure 2. **Visualizing the self-supervised representation space:** The top panel shows a heatmap of SimCLR representations of random ImageNet-1K samples. In the second panel, we plot the distribution of the features of the visualized samples for various models. We observe that representations are mostly sparse with a small number of strongly activated coordinates.

3.1. Discriminative Features

Based on Figure 1, we can define three broad categories of highly activating features: (i) Features that are highly activating across a very small fraction of the population, corresponding to the lower tail features in Figure 1. We take the example of features 621, 251 and 1021 and visualize their highly activating samples and gradient heatmaps (using GradCAM [39]). Since these features activate very

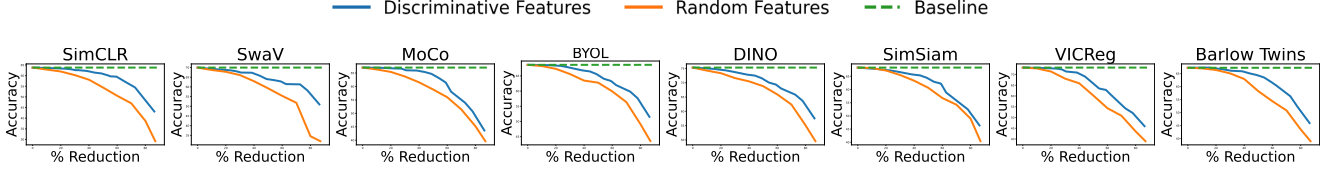


Figure 3. **Linear classification accuracy on discriminative features:** We train linear classifiers after selecting subsets of discriminative features of various sizes (middle portion of Figure 1) and plot their top-1 accuracy for various self-supervised baselines. We compare these results to the baseline and the accuracy on randomly selected features of matching sizes (averaged over 4 random seeds). Classifiers trained using discriminative features consistently outperform those of randomly selected features. We can achieve up to 40% reduction in representations size using discriminative features without significantly affecting the top-1 accuracy.

few samples, they likely correspond to image-specific or uncommon attributes. Such features would also not be useful in classification tasks as these are not shared, class-relevant attributes. (ii) Features that highly activate a very large number of samples in the population i.e. the upper tail features in Figure 1. Like feature 2021 and 401, such features are likely to encode very broad and general characteristics (like texture, color etc.) common to most samples (spanning various classes) and therefore, are not class-discriminative. The third category includes, (iii) Features that are highly activating across a moderate number of samples in the population (i.e. the middle part in Figure 1). These features are most likely to encode unique physical attributes associated with particular classes. For example, feature 98 corresponds to the “stripe” pattern which is an important property of the zebra class. Similarly, feature 970 corresponds to the style of the daisy class, and feature 1266 corresponds to water fountains in different scenes. We refer to this subset of highly activating features as *discriminative features*. Note that we did not use any label information for this analysis. We can identify discriminative and non-discriminative features in a fully unsupervised manner by simply observing their percentage activations (A). The bar plots in Figure 1, show that these features activate more than 80% of particular classes which confirms that these features are strongly class-correlated.

We justify the described method of selection in Figure 3, where we plot the top-1 accuracy of a linear classifier trained on ImageNet-1K using subsets of discriminative features of varying sizes as chosen from Figure 1 (middle portion). We also plot the top-1 accuracy when random subsets of features are selected. We observe that discriminative features perform significantly better compared to randomly selected features. We also observe that we can reduce the representation size up to 40% using the discriminative features, with minimal reduction in performance. In practice, for a given model and dataset, we find that the discriminative features selected between the 55th and the 97th percentile of A (as shown in Figure 1), consistently gives us the best performance. Since our analysis assumes that highly activating features are axis-aligned, we also perform a PCA

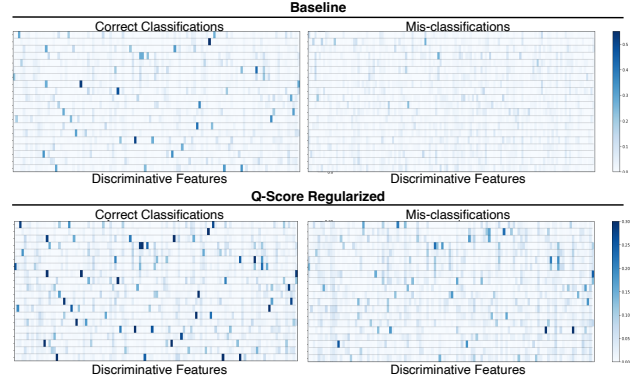


Figure 4. **Comparing correct and mis-classified representations:** In these heatmaps, we visualize the discriminative features of average SimCLR representations of several ImageNet-1K classes - correct (left) and incorrect (right) classifications. In the baseline, we observe that discriminative features are strongly activated only in correctly classified representations. Q-Score regularization improves discriminative features’ activations, even in mis-classified representations.

analysis on the representation space (see Appendix) to partially validate this assumption. We show that the gradient heatmaps of the highly activating features are strongly correlated with that of highly activating PCA features. Moreover, we show that discriminative features and PCA features perform comparably in downstream linear evaluation, up to 40% reduction in representation size.

3.2. Mis-classified Representations

We now study how discriminative features play a key role in detecting potential mis-classifications in a fully unsupervised manner, without requiring to train a linear classification head. In Figure 4, we take SimCLR ImageNet-1K representations and visualize the discriminative features. On the left, we show the average representations of correctly classified samples in a subset of classes, while on the right, we show the same for the mis-classified samples in those classes. The subset of features we display is the same for correct and incorrect classifications.

As we can see, in Figure 4, in the first panel, there is a clear difference between representations of correctly

and incorrectly classified examples. Both correct and misclassified representations are *nearly* sparse, however, the discriminative features are significantly more activated in correct classifications. This is especially interesting because we can visually distinguish between correct and incorrect classifications, just by observing the discriminative features, without using any label information.

The correlation of discriminative features to unique physical attributes as studied in Section 3.1, suggests that their presence may be useful in correctly classifying representations. In Figure 4, our claim is confirmed as we observe that mis-classified representations do not show high activations on these features. Therefore, for any given sample, we can consider discriminative features as strong signals indicating classification outcome. We would like to emphasize that our results only indicate an *association* between these structural properties and classification accuracy and we do not claim any causal relationship between the two. In the next Section 4, we show that enhancing these properties, through regularization, improves the overall quality of representations, followed by improved classification accuracy and interpretability.

4. Self-Supervised Representation Q-Score

Our study of learned representation patterns helps us discover discriminative features in an unsupervised manner. Discriminative features commonly activate class-specific attributes and help us visually distinguish between correct and incorrect classifications. We combine these observations to design a sample-wise quality score for self-supervised representations. Let us define D , such that $|D| < r$, as the set of discriminative features for a given self-supervised model trained on a given dataset. For the i^{th} sample, we have \mathbf{h}_i (representation), μ_i (mean of \mathbf{h}_i), σ_i (standard deviation of \mathbf{h}_i) and the set of highly activating features $L_i = \{j : h_{ij} > \mu_i + \epsilon\sigma_i\}, |L_i| < r$. We define our Self-Supervised Quality Score for sample i as,

$$Q_i := \frac{1}{|L_i \cap D|} \sum_{j \in L_i \cap D} (h_{ij} - \mu_i) \quad (1)$$

where, $L_i \cap D$ is the set of discriminative features specific to the i^{th} sample. Intuitively, higher Q_i implies that the representation contains highly activated discriminative features which are strongly deviated from the mean. Our objective with this metric is to compute a sample-specific score in an unsupervised manner indicating the quality of its representations. Ideally, we would like to argue that samples with higher Q-score have improved representations and thus are more likely to be classified correctly in the downstream task. This is a general score that can be applied to any self-supervised model trained on any dataset. See Appendix for a discussion on Q-Score in supervised models.

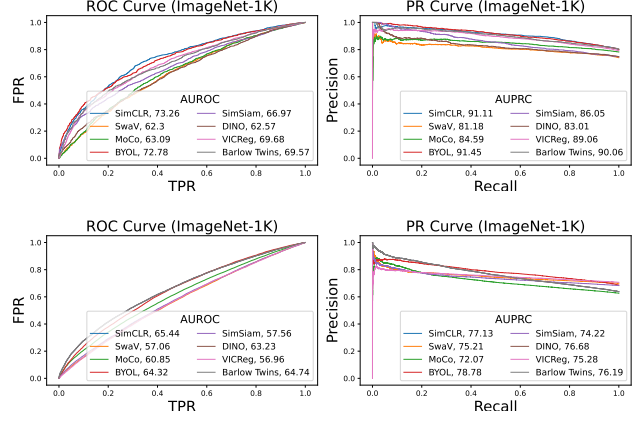


Figure 5. **Precision-Recall and ROC curves of Q-Score:** We measure the effectiveness of Q-Score when used as a predictor in distinguishing between correct and mis-classified representations on ImageNet-100 and ImageNet-1K on each self-supervised model. Q-Score shows an AUPRC of up to 91.45 on ImageNet-100, 78.78 on ImageNet-1K and AUROC of 73.26 on ImageNet-100, 65.44 on ImageNet-1K.

Next, we measure how effective our score is in differentiating between correctly and incorrectly classified representations in an unsupervised manner. In Figure 5, we plot the Precision-Recall (PR) curve and the Receiver Operating Characteristic (ROC) curve of Q-Score when used as a predictor of classification outcome (correct or incorrect). We show this for SimCLR, SwaV, MoCo, BYOL, DINO and SimSiam for the validation set of ImageNet-100 containing 5000 samples (top panel) and ImageNet-1K containing 50000 samples (bottom panel). We also compute the AUROC (area under receiver operating characteristic curve) and AUPRC (area under precision-recall curve) of these curves. We observe AUPRC up to 91.45 on ImageNet-100 and 78.78 on ImageNet-1K on BYOL. On SimCLR, we observe AUROC up to 73.26 on ImageNet-100 and 65.44 on ImageNet-1K. Based on these results we can conclude that, Q-Score is a reliable metric in assessing the quality of representations, meaning that representations with lower Q-Score (quality), are more likely to be mis-classified.

We now check if promoting Q-Score on pre-trained representations is helpful. To do so, we take state-of-the-art pre-trained self-supervised models and further train them for a small number of iterations with Q-Score as a regularizer. For example, we can apply this regularizer to the SimCLR optimization as follows,

$$\max_{\theta} \frac{1}{2N} \sum_{i=1}^{2N} \left[\log \frac{\text{sim}(\mathbf{z}_i, \tilde{\mathbf{z}}_i)}{\sum_{j=1}^{2N} \mathbb{1}_{j \neq i} \text{sim}(\mathbf{z}_i, \mathbf{z}_j)} + \lambda_1 \mathbb{1}_{Q_i < \alpha}(Q_i) \right] \quad (2)$$

where \mathbf{z} is the latent vector computed by passing \mathbf{h}

Table 1. **Boosting linear classification performance with Q-Score regularization:** We tabulate the top-1 accuracy of linear evaluation on SimCLR [13], SwaV [11], MoCo [14], BYOL [26], DINO [12], SimSiam [15], VICReg [3] and Barlow Twins [49] with and without Q-Score regularized fine-tuning. We also compare with a simple lasso regularization [42]. We observe that Q-Score regularization consistently improves each self-supervised state-of-the-art baseline achieving up to 5.8% relative improvement on ImageNet-100 and 3.7% on ImageNet-1K.

Model	ImageNet-100			ImageNet-1K		
	Baseline	Lasso	Q-Score	Baseline	Lasso	Q-Score
SimCLR	78.64	75.63	80.79 (+2.2%)	63.80	61.48	66.18 (+2.3%)
SwaV	74.36	74.56	78.90 (+4.5%)	69.95	67.35	71.05 (+1.1%)
MoCo	79.62	78.81	85.16 (+5.5%)	67.03	65.12	69.31 (+2.2%)
BYOL	80.88	78.73	86.72 (+5.8%)	69.14	68.47	72.81 (+3.7%)
DINO	75.41	75.18	76.39 (+1.0%)	75.52	72.89	75.78 (+0.3%)
SimSiam	78.80	78.42	81.41 (+2.6%)	68.62	68.63	70.47 (+1.9%)
VICReg	79.77	76.95	81.56 (+1.8%)	73.63	72.86	74.72 (+1.1%)
Barlow	80.63	80.32	81.03 (+0.4%)	67.85	66.47	69.58 (+1.7%)

through a projector network and $\text{sim}(\cdot)$ denotes the exponentiated cosine similarity of the normalized latent vector. α is a threshold with which we select the low-score samples whose Q-Scores should be maximized and λ_1 is the regularization coefficient. In other words the goal of this regularization is to improve low-quality representations, similar to the ones shown in Figure 4, by maximizing their discriminative features for downstream classification.

In practice, directly applying this regularization could lead to a trivial solution where a small set of features gets activated for all samples. This is not a favorable situation because these representations become harder to classify accurately and more importantly, the discriminative features are no longer *informative* because they are activated for all samples (similar to the upper tail in Figure 1). Such features have significantly large L1 norms *across* samples compared to the remaining features. Therefore, in our revised optimization, we penalize features that have large L1 norms across samples. Let us denote the representation matrix of a given batch by $\mathbf{H} \in \mathbb{R}^{2N \times r}$ and $\|\mathbf{H}_{*,k}\|_1$ represents the L1 norm of the k^{th} column (corresponding to the k^{th} feature). Our regularized objective would then be,

$$\max_{\theta} \frac{1}{2N} \sum_{i=1}^{2N} \left[\log \frac{\text{sim}(\mathbf{z}_i, \tilde{\mathbf{z}}_i)}{\sum_{j=1}^{2N} \mathbb{1}_{j \neq i} \text{sim}(\mathbf{z}_i, \mathbf{z}_j)} + \lambda_1 \mathbb{1}_{Q_i < \alpha}(Q_i) \right] - \lambda_2 \sum_{k=1}^r \mathbb{1}_{\|\mathbf{H}_{*,k}\|_1 > \beta} (\|\mathbf{H}_{*,k}\|_1) \quad (3)$$

where the threshold β helps us select the uninformative features whose L1 norms should be minimized. In practice, we choose α and β for each batch as the mean values of Q_i and $\|\mathbf{H}_{*,k}\|_1$ respectively.

4.1. Experimental Setup

Our setup consists of state-of-the-art self-supervised ResNet encoders ($f(\cdot)$) - SimCLR [13], SwaV [11], MoCo [14], BYOL [26], DINO [12] (ResNet-based), SimSiam [15], VICReg [3] and Barlow Twins [49] that are pre-trained on datasets - ImageNet-1K [38], ImageNet-100 [38]. We use a ResNet-50 encoder for our ImageNet-1K experiments and ResNet-18 encoder for all other datasets. We discover discriminative features for each pre-trained model using the validation set of each dataset. For Q-Score regularization, maintaining the same encoder architecture as the respective papers, we use the LARS [48] optimizer with warmup-anneal scheduling. We fine-tune each pre-trained model with and without Q-Score regularization (controlled by λ_1 and λ_2) using a low learning rate of 10^{-5} , until convergence (which takes up to 50 epochs). We find that $\lambda_1 = \lambda_2 = 10^{-4}$ generally works well for fine tuning. We use a maximum of 4 NVIDIA RTX A4000 GPUs (16GB memory) for all our experiments. Using the implementations from solo-learn [18], we have tried to match our baseline numbers as much as possible within the error bars reported in the papers using the available resources. We perform standard linear evaluation by passing frozen pre-trained representations through a linear classifier that predicts class labels. For all our gradient heatmap visualizations, we utilize GradCAM [39].

4.2. Q-Score Regularization

We tabulate our linear evaluation results of various self-supervised baselines before and after Q-Score regularization in Table 1. We also include results on lasso (L1) regularization [42] on pre-trained models. Lasso promotes sparsity by minimizing the L1 norm of representations. Q-Score regularization improves the linear probing top-1 accuracy on all of the self-supervised state-of-the-art models. We observe the most improvement on BYOL showing 5.8% increase in accuracy on ImageNet-100 and 3.7% on ImageNet-1K. Lasso regularization shows degraded performance across most models since naively sparsifying representations can lead to loss of information. In contrast, Q-Score regularization promotes highly activating discriminative coordinates which we have shown to be essential for downstream classification. We include more results on CIFAR-10 [34], STL-10 [17] and CIFAR-100 [35] in the Appendix. We also include the results on the transfer performance of discriminative features and Q-Score regularized ImageNet-1K models on unseen datasets in the appendix. Q-Score is therefore a powerful regularizer that can boost the performance of state-of-the-art self-supervised baselines.

In addition to top-1 accuracy, Q-Score also shows significant improvement in representation quality. In Figure 4, we compare the discriminative features of representa-

tions before and after Q-Score regularization. We observe that the magnitude of discriminative features increases with Q-Score regularization on both correct and mis-classified representations. We also observe improved classification confidence as representations become more disentangled (see Appendix for a discussion on this). Our regularization produces better quality representations with clear discriminative features making them more distinguishable across classes and therefore, easier to classify. Due to this, we can attribute the improvement in performance to improved representation quality. Although Q-Score improves accuracy, it does not entirely prevent mis-classifications as mis-classifications may occur due to a variety of reasons such as, hardness of samples, encoder capacity, dataset imbalance etc.

Our motivation for using discriminative features as discussed in Section 3 is because - a) they are at clear contrast between correct and incorrect classifications, and b) they show strong correlation to ground truth. We observed in Figure 4 in the baseline, that the discriminative features in correctly classified samples are not strongly activated in mis-classified samples. We now study some mis-classified samples and observe how their features may improve with Q-Score regularization. In Figure 6, we visualize the gradient heatmaps of the discriminative features of some mis-classified examples in SimCLR. In the baseline, we observe that discriminative features do highlight portions of the image relevant to the ground truth, however, they may also activate other portions that are not necessarily important (see rock crab and green mamba). These heatmaps reflect low quality representations where the discriminative features are not strongly deviated from the mean. After Q-Score regularization, the maximization of discriminative features also leads to better gradient heatmaps that are more localized and cover almost all important portions of the image relevant to the ground truth. Therefore, these samples get classified correctly with higher confidence after regularization.

5. Quantifying Representation Interpretability with Salient ImageNet

We have observed that discriminative features in representations correspond to meaningful physical attributes through gradient heatmaps and they play a key role in deciding the downstream classification outcome. In this section, we quantify the interpretability of these features between correct and incorrect classifications. We utilize Salient ImageNet [40] as the ground truth baseline to compare our gradient heatmaps with. The Salient ImageNet dataset contains annotated masks for both "core" and "spurious" features extracted from a supervised robust ResNet-50 model for 6858 images spanning 327 ImageNet classes. It also contains some natural language keywords, provided by workers to explain each feature. Core features are those that are highly

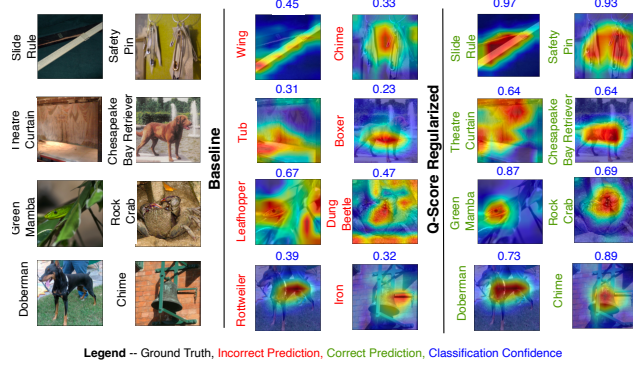


Figure 6. **Discriminative features in mis-classified samples:** The discriminative features’ heatmaps on the SimCLR (baseline) activate portions that may not be relevant to the image ground truth, leading to incorrect predictions. After Q-Score regularization on these representations, the heatmaps become more localized and less noisy, whilst improving predictions and confidence.

correlated with the ground truth of the image, whereas, spurious features are those that activate portions irrelevant to the ground truth. In Figure 7, we study some correct and mis-classified samples in the SimCLR baseline. We plot the gradient heatmaps of the discriminative features (combining each individual feature heatmap) of SimCLR for each respective image. We also plot the core and spurious masks of the same images from the Salient ImageNet dataset. We observe that discriminative SimCLR features mostly capture relevant and defining characteristics of the images, therefore are highly correlated with the ground-truth. Moreover, for every correctly classified image, these heatmaps overlap more with core features than spurious features in Salient ImageNet. discriminative features in mis-classified images also overlap with core features in most cases. Since discriminative features are very closely related (in terms of overlap) to *core* features, we can potentially explain these features better with the help of worker annotations in Salient ImageNet. Therefore, these features can be considered as *interpretable*.

We quantitatively measure the interpretability of a given representation of a given model by computing the Intersection over Union (mIoU) between the heatmap of discriminative features and the core or spurious mask of that image in Salient ImageNet. We can extend this to measure the overall interpretability of a given model by computing the mean Intersection over Union (mIoU) over the population. For the i^{th} image, we define Ar_i as the area of the heatmap of its discriminative features. Let Ar_i^{core} and Ar_i^{sp} be the area of the core and spurious masks respectively. The mIoU scores are defined as follows,

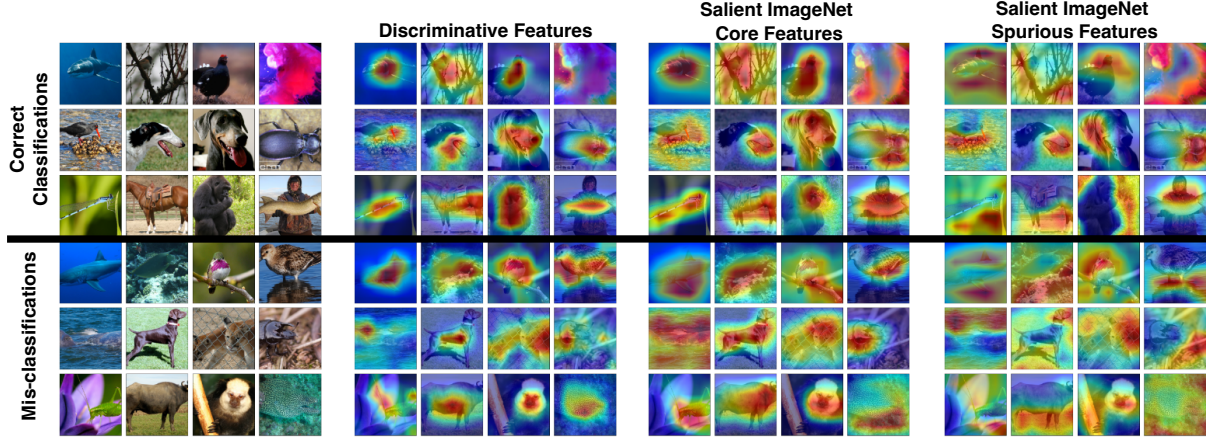


Figure 7. **Comparing discriminative features with Salient ImageNet core and spurious features:** We compare the gradient heatmaps of discriminative features correct and incorrect classifications of SimCLR on ImageNet-1K with the core and spurious masks of the same images in Salient ImageNet [40]. We observe that discriminative features generally overlap more with core features in Salient ImageNet.

$$\text{mIoU}^{\text{core}} = \frac{1}{N} \sum_i \frac{s(Ar_i \cap Ar_i^{\text{core}})}{s(Ar_i \cup Ar_i^{\text{core}})}$$

$$\text{mIoU}^{\text{sp}} = \frac{1}{N} \sum_i \frac{s(Ar_i \cap Ar_i^{\text{sp}})}{s(Ar_i \cup Ar_i^{\text{sp}})}$$

where $s(\cdot)$ calculates the sum of the pixel values of the discriminative features’ heatmap in the given area. Higher $\text{mIoU}^{\text{core}}\%$ indicates that, on an average higher percentage of the feature heatmap overlaps with the annotated core region, meaning that the model features are more interpretable.

In Figure 8, we show that for all self-supervised baselines, $\text{mIoU}^{\text{core}} > \text{mIoU}^{\text{sp}}$ for both correct and incorrect classifications which confirms that discriminative features generally encode important and core attributes over the whole population. Among correct and mis-classified samples in the baselines, we observe that the $\text{mIoU}^{\text{core}}$ of correct classifications is higher than mis-classifications. This aligns with our observations in Figure 6, which shows that discriminative features in mis-classified samples may not be strongly deviated from the mean and therefore, may correspond to less important portions of the image. After Q-Score regularization, we observe an increase in $\text{mIoU}^{\text{core}}$ for both correct and mis-classified samples compared to the baseline. This shows that our regularization which enhances discriminative features produces better gradient heatmaps which are more overlapped with core portions of images and therefore, improves the overall model interpretability.

6. Conclusion

We studied the representation space of self-supervised models to identify discriminative features, a subset of features that correspond to unique physical attributes and show

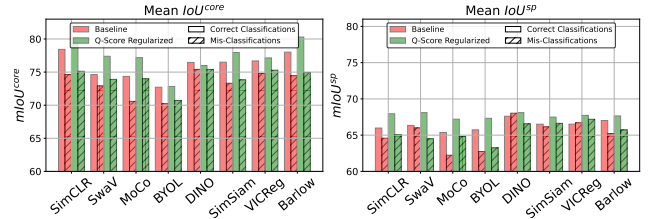


Figure 8. **mIoU scores with core and spurious Salient ImageNet features:** We compute the mean $\text{mIoU}^{\text{core}}$ and mIoU^{sp} scores of SSL baselines (using their discriminative features) before and after Q-Score regularization. We observe that discriminative features for all models generally show higher % IoU with core features than spurious features. Mis-classified representations show relatively lower % IoU with core features. After Q-score regularization, we observe that $\text{mIoU}^{\text{core}}$ generally improves for both correct and mis-classified representations.

strong class-correlation although they are selected in a fully unsupervised manner. Using discriminative features, we can compress the representation space by up to 40% without affecting the downstream linear evaluation performance to a large extent. Moreover, discriminative features are more strongly activated in correct classifications compared to mis-classified ones. Building on these observations, we define an unsupervised sample-wise score, Self-Supervised Representation Quality Score (Q-Score) that is effective in determining how likely samples are to be correctly or incorrectly classified. With the help of Q-Score regularization during pre-training, we remedied low-quality samples by improving their Q-Scores, thereby, improving the overall accuracy of state-of-the-art self-supervised models on ImageNet-1K by up to 3.7%. We also quantify representation interpretability with an IoU metric using Salient ImageNet masks as ground truth. With this metric, we confirm

that highly activating features are more overlapped with core attributes. We also observed that regularization improves over model interpretability due to enhancing highly activating features. Our paper poses important questions for future studies such as: 1) what are the causes of misclassifications, apart from representation quality, 2) how can we better explain self-supervised features, given that there are no labels, 3) how can we utilize the better representations space for other tasks besides classification.

References

- [1] Sanjeev Arora, Hrishikesh Khandeparkar, Mikhail Khodak, Orestis Plevrakis, and Nikunj Saunshi. A theoretical analysis of contrastive unsupervised representation learning, 2019. [3](#)
- [2] Philip Bachman, R Devon Hjelm, and William Buchwalter. Learning representations by maximizing mutual information across views. In H. Wallach, H. Larochelle, A. Beygelzimer, F. d'Alché-Buc, E. Fox, and R. Garnett, editors, *Advances in Neural Information Processing Systems*, volume 32. Curran Associates, Inc., 2019. [3](#)
- [3] Adrien Bardes, Jean Ponce, and Yann LeCun. Vircreg: Variance-invariance-covariance regularization for self-supervised learning, 2021. [1](#), [3](#), [6](#)
- [4] Miguel A Bautista, Artsiom Sanakoyeu, Ekaterina Tikhoncheva, and Bjorn Ommer. Cliqecnn: Deep unsupervised exemplar learning. In D. Lee, M. Sugiyama, U. Luxburg, I. Guyon, and R. Garnett, editors, *Advances in Neural Information Processing Systems*, volume 29. Curran Associates, Inc., 2016. [2](#)
- [5] Piotr Bojanowski and Armand Joulin. Unsupervised learning by predicting noise. In Doina Precup and Yee Whye Teh, editors, *Proceedings of the 34th International Conference on Machine Learning*, volume 70 of *Proceedings of Machine Learning Research*, pages 517–526. PMLR, 06–11 Aug 2017. [2](#)
- [6] Florian Bordes, Randall Balestriero, and Pascal Vincent. High fidelity visualization of what your self-supervised representation knows about, 2021. [3](#)
- [7] Lukas Bossard, Matthieu Guillaumin, and Luc Van Gool. Food-101 – mining discriminative components with random forests. In *European Conference on Computer Vision*, 2014. [12](#), [13](#)
- [8] Mathilde Caron, Piotr Bojanowski, Armand Joulin, and Matthijs Douze. Deep clustering for unsupervised learning of visual features. *Lecture Notes in Computer Science*, page 139–156, 2018. [1](#)
- [9] Mathilde Caron, Piotr Bojanowski, Armand Joulin, and Matthijs Douze. Deep clustering for unsupervised learning of visual features. In *Proceedings of the European Conference on Computer Vision (ECCV)*, September 2018. [2](#)
- [10] Mathilde Caron, Piotr Bojanowski, Julien Mairal, and Armand Joulin. Unsupervised pre-training of image features on non-curated data. In *Proceedings of the IEEE/CVF International Conference on Computer Vision (ICCV)*, October 2019. [2](#)
- [11] Mathilde Caron, Ishan Misra, Julien Mairal, Priya Goyal, Piotr Bojanowski, and Armand Joulin. Unsupervised learning of visual features by contrasting cluster assignments. In H. Larochelle, M. Ranzato, R. Hadsell, M. F. Balcan, and H. Lin, editors, *Advances in Neural Information Processing Systems*, volume 33, pages 9912–9924. Curran Associates, Inc., 2020. [1](#), [3](#), [6](#)
- [12] Mathilde Caron, Hugo Touvron, Ishan Misra, Hervé Jégou, Julien Mairal, Piotr Bojanowski, and Armand Joulin. Emerging properties in self-supervised vision transformers. In *Proceedings of the IEEE/CVF International Conference on Computer Vision (ICCV)*, pages 9650–9660, October 2021. [1](#), [3](#), [6](#)
- [13] Ting Chen, Simon Kornblith, Mohammad Norouzi, and Geoffrey Hinton. A simple framework for contrastive learning of visual representations. In Hal Daumé III and Aarti Singh, editors, *Proceedings of the 37th International Conference on Machine Learning*, volume 119 of *Proceedings of Machine Learning Research*, pages 1597–1607. PMLR, 13–18 Jul 2020. [1](#), [2](#), [3](#), [6](#)
- [14] Xinlei Chen, Haoqi Fan, Ross Girshick, and Kaiming He. Improved baselines with momentum contrastive learning, 2020. [1](#), [3](#), [6](#)
- [15] Xinlei Chen and Kaiming He. Exploring simple siamese representation learning. In *Proceedings of the IEEE/CVF Conference on Computer Vision and Pattern Recognition (CVPR)*, pages 15750–15758, June 2021. [1](#), [3](#), [6](#)
- [16] M. Cimpoi, S. Maji, I. Kokkinos, S. Mohamed, , and A. Vedaldi. Describing textures in the wild. In *Proceedings of the IEEE Conf. on Computer Vision and Pattern Recognition (CVPR)*, 2014. [12](#)
- [17] Adam Coates, Honglak Lee, and Andrew Y. Ng. Stanford stl-10 image dataset. *AISTATS*, 2011. [6](#), [11](#), [12](#)
- [18] Victor Guilherme Turrissi da Costa, Enrico Fini, Moin Nabi, Nicu Sebe, and Elisa Ricci. solo-learn: A library of self-supervised methods for visual representation learning. *Journal of Machine Learning Research*, 23(56):1–6, 2022. [6](#)
- [19] Alexey Dosovitskiy, Philipp Fischer, Jost Tobias Springenberg, Martin Riedmiller, and Thomas Brox. Discriminative unsupervised feature learning with exemplar convolutional neural networks. *IEEE Transactions on Pattern Analysis and Machine Intelligence*, 38(9):1734–1747, 2016. [2](#)
- [20] Alexey Dosovitskiy, Jost Tobias Springenberg, Martin Riedmiller, and Thomas Brox. Discriminative unsupervised feature learning with convolutional neural networks. In Z. Ghahramani, M. Welling, C. Cortes, N. Lawrence, and K. Q. Weinberger, editors, *Advances in Neural Information Processing Systems*, volume 27. Curran Associates, Inc., 2014. [2](#)
- [21] Debidatta Dwibedi, Yusuf Aytar, Jonathan Tompson, Pierre Sermanet, and Andrew Zisserman. With a little help from my friends: Nearest-neighbor contrastive learning of visual representations. *2021 IEEE/CVF International Conference on Computer Vision (ICCV)*, Oct 2021. [3](#)
- [22] Logan Engstrom, Andrew Ilyas, Shibani Santurkar, Dimitris Tsipras, Brandon Tran, and Aleksander Madry. Adversarial robustness as a prior for learned representations, 2020. [12](#)

- [23] Linus Ericsson, Henry Gouk, and Timothy M. Hospedales. Why do self-supervised models transfer? investigating the impact of invariance on downstream tasks, 2021. [1](#)
- [24] Quentin Garrido, Randall Balestriero, Laurent Najman, and Yann Lecun. Rankme: Assessing the downstream performance of pretrained self-supervised representations by their rank, 2022. [3](#)
- [25] Tom George Grigg, Dan Busbridge, Jason Ramapuram, and Russ Webb. Do self-supervised and supervised methods learn similar visual representations?, 2021. [3](#)
- [26] Jean-Bastien Grill, Florian Strub, Florent Althé, Corentin Tallec, Pierre Richemond, Elena Buchatskaya, Carl Doersch, Bernardo Avila Pires, Zhaohan Guo, Mohammad Gheshlaghi Azar, Bilal Piot, koray kavukcuoglu, Remi Munos, and Michal Valko. Bootstrap your own latent - a new approach to self-supervised learning. In H. Larochelle, M. Ranzato, R. Hadsell, M. F. Balcan, and H. Lin, editors, *Advances in Neural Information Processing Systems*, volume 33, pages 21271–21284. Curran Associates, Inc., 2020. [1](#), [3](#), [6](#)
- [27] Kaiming He, Xiangyu Zhang, Shaoqing Ren, and Jian Sun. Deep residual learning for image recognition. In *2016 IEEE Conference on Computer Vision and Pattern Recognition (CVPR)*, pages 770–778, 2016. [2](#), [3](#)
- [28] Jiabo Huang, Qi Dong, Shaogang Gong, and Xiatian Zhu. Unsupervised deep learning by neighbourhood discovery. In Kamalika Chaudhuri and Ruslan Salakhutdinov, editors, *Proceedings of the 36th International Conference on Machine Learning*, volume 97 of *Proceedings of Machine Learning Research*, pages 2849–2858. PMLR, 09–15 Jun 2019. [2](#)
- [29] Weiran Huang, Mingyang Yi, and Xuyang Zhao. Towards the generalization of contrastive self-supervised learning, 2021. [1](#)
- [30] Li Jing, Pascal Vincent, Yann LeCun, and Yuandong Tian. Understanding dimensional collapse in contrastive self-supervised learning. In *International Conference on Learning Representations*, 2022. [1](#), [3](#)
- [31] Prannay Khosla, Piotr Teterwak, Chen Wang, Aaron Sarna, Yonglong Tian, Phillip Isola, Aaron Maschinot, Ce Liu, and Dilip Krishnan. Supervised contrastive learning, 2020. [1](#), [3](#)
- [32] Soroush Abbasi Koohpayegani, Ajinkya Tejankar, and Hamed Pirsiavash. Mean shift for self-supervised learning. *2021 IEEE/CVF International Conference on Computer Vision (ICCV)*, Oct 2021. [3](#)
- [33] Jonathan Krause, Michael Stark, Jia Deng, and Li Fei-Fei. 3d object representations for fine-grained categorization. In *4th International IEEE Workshop on 3D Representation and Recognition (3D-RR-13)*, Sydney, Australia, 2013. [12](#), [13](#)
- [34] Alex Krizhevsky, Vinod Nair, and Geoffrey Hinton. Cifar-10 (canadian institute for advanced research). 2009. [6](#), [11](#), [12](#)
- [35] Alex Krizhevsky, Vinod Nair, and Geoffrey Hinton. Cifar-100 (canadian institute for advanced research). 2009. [6](#), [11](#), [12](#)
- [36] S. Maji, J. Kannala, E. Rahtu, M. Blaschko, and A. Vedaldi. Fine-grained visual classification of aircraft. Technical report, 2013. [12](#), [13](#)
- [37] Maria-Elena Nilsback and Andrew Zisserman. Automated flower classification over a large number of classes. In *Indian Conference on Computer Vision, Graphics and Image Processing*, Dec 2008. [12](#), [13](#), [14](#)
- [38] Olga Russakovsky, Jia Deng, Hao Su, Jonathan Krause, Sanjeev Satheesh, Sean Ma, Zhiheng Huang, Andrej Karpathy, Aditya Khosla, Michael Bernstein, Alexander C. Berg, and Li Fei-Fei. ImageNet Large Scale Visual Recognition Challenge. *International Journal of Computer Vision (IJCV)*, 115(3):211–252, 2015. [3](#), [6](#)
- [39] Ramprasaath R. Selvaraju, Michael Cogswell, Abhishek Das, Ramakrishna Vedantam, Devi Parikh, and Dhruv Batra. Grad-cam: Visual explanations from deep networks via gradient-based localization. *International Journal of Computer Vision*, 128(2):336–359, Oct 2019. [3](#), [6](#)
- [40] Sahil Singla and Soheil Feizi. Salient imagenet: How to discover spurious features in deep learning?, 2021. [2](#), [7](#), [8](#), [12](#)
- [41] Yonglong Tian, Chen Sun, Ben Poole, Dilip Krishnan, Cordelia Schmid, and Phillip Isola. What makes for good views for contrastive learning? In H. Larochelle, M. Ranzato, R. Hadsell, M. F. Balcan, and H. Lin, editors, *Advances in Neural Information Processing Systems*, volume 33, pages 6827–6839. Curran Associates, Inc., 2020. [3](#)
- [42] Robert Tibshirani. Regression shrinkage and selection via the lasso. *Journal of the Royal Statistical Society: Series B (Methodological)*, 58(1):267–288, 1996. [6](#)
- [43] Christopher Tosh, Akshay Krishnamurthy, and Daniel Hsu. Contrastive learning, multi-view redundancy, and linear models, 2021. [3](#)
- [44] J. von Kügelgen*, Y. Sharma*, L. Gresele*, W. Brendel, B. Schölkopf, M. Besserve, and F. Locatello. Self-supervised learning with data augmentations provably isolates content from style. In *Advances in Neural Information Processing Systems 34 (NeurIPS 2021)*, Dec. 2021. *equal contribution. [3](#)
- [45] Zhirong Wu, Yuanjun Xiong, Stella X. Yu, and Dahua Lin. Unsupervised feature learning via non-parametric instance discrimination. In *Proceedings of the IEEE Conference on Computer Vision and Pattern Recognition (CVPR)*, June 2018. [2](#)
- [46] Tete Xiao, Xiaolong Wang, Alexei A Efros, and Trevor Darrell. What should not be contrastive in contrastive learning. In *International Conference on Learning Representations*, 2021. [3](#)
- [47] Asano YM., Rupprecht C., and Vedaldi A. Self-labelling via simultaneous clustering and representation learning. In *International Conference on Learning Representations*, 2020. [2](#)
- [48] Yang You, Igor Gitman, and Boris Ginsburg. Large batch training of convolutional networks. *arXiv: Computer Vision and Pattern Recognition*, 2017. [6](#)
- [49] Jure Zbontar, Li Jing, Ishan Misra, Yann LeCun, and Stéphane Deny. Barlow twins: Self-supervised learning via redundancy reduction, 2021. [1](#), [3](#), [6](#)

Table A.1. **Linear classification performance with Q-Score regularization (more datasets):** Similar to Table 1, we tabulate our results on CIFAR-10 [34], CIFAR-100 [35] and STL-10 [17]

Model	CIFAR-10			CIFAR-100			STL-10		
	Baseline	Lasso	Q-Score	Baseline	Lasso	Q-Score	Baseline	Lasso	Q-Score
SimCLR	90.83	89.33	92.31	65.82	68.21	68.90	76.42	75.59	79.83
SwaV	89.23	89.37	90.03	65.13	66.06	66.52	73.94	69.93	75.03
MoCo	92.95	90.59	94.77	70.12	67.23	71.16	73.21	72.65	74.29
BYOL	92.59	90.27	92.82	70.54	71.26	72.71	70.59	70.27	74.47
DINO	89.54	89.57	89.85	66.82	65.52	67.49	68.36	69.29	69.38
SimSiam	91.03	90.74	92.48	66.58	65.69	69.03	72.94	67.54	73.52
VICReg	92.69	91.83	93.74	68.81	66.75	71.76	70.76	70.61	72.82
Barlow	93.46	91.75	93.87	71.82	71.54	71.91	74.17	70.27	74.32

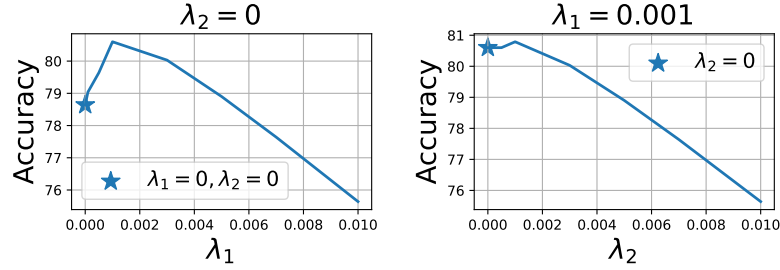


Figure A.1. **Hyper-parameter Search on λ_1 and λ_2 :** We set $\lambda_2 = 0$ and search across various values of λ_1 to find the best performing experiment. Next, we set λ_1 to the best performing value and search over λ_2 .

A. Appendix

A.1. Results on Other Datasets

As an extension to the results shown in Table 1, we include results on more datasets including CIFAR-10 [34], CIFAR-100 [35] and STL-10 [17] on 8 self-supervised baselines when fine-tuned (further trained) with and without Q-Score regularization. In Table A.2, we observe that Q-Score regularization helps boost the performance of all state-of-the-art models across datasets.

A.2. Ablation on λ_1 and λ_2

In this section, we discuss how we can perform a hyper-parameter search on λ_1 and λ_2 to find the best performing pair of values. We take the baseline of SimCLR trained on ImageNet-1K and further train this model under the setup outlined in Section 4.1. We train keeping both $\lambda_1 = \lambda_2 = 0$ and run experiments by gradually increasing λ_1 to find the best performing value. Next, we search over λ_2 keeping the best performing value of λ_1 . In these experiments we find that $\lambda_1 = \lambda_2 = 10^{-4}$ is the best performing pair. We find that this pair shows improved performance across most experiments. Due to lack of resources, we do not heavily tune these hyper-parameters in our experiments, however, we can expect improved performance if tuning is performed.

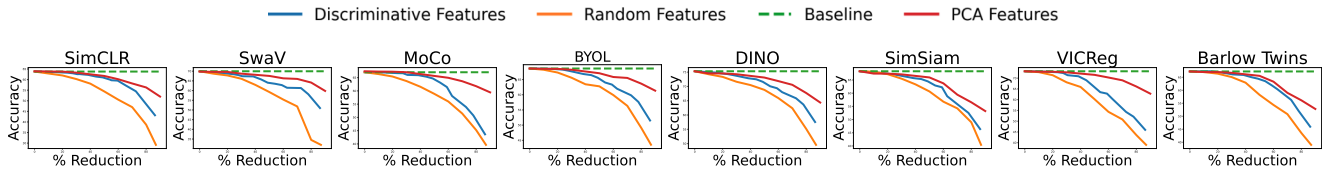


Figure A.2. **Linear classification accuracy on discriminative features:** Similar to Figure 3, we compare discriminative and random features to PCA features of matching sizes. Discriminative features also match the performance of PCA features to a certain extent showing that features can be considered as axis-aligned.

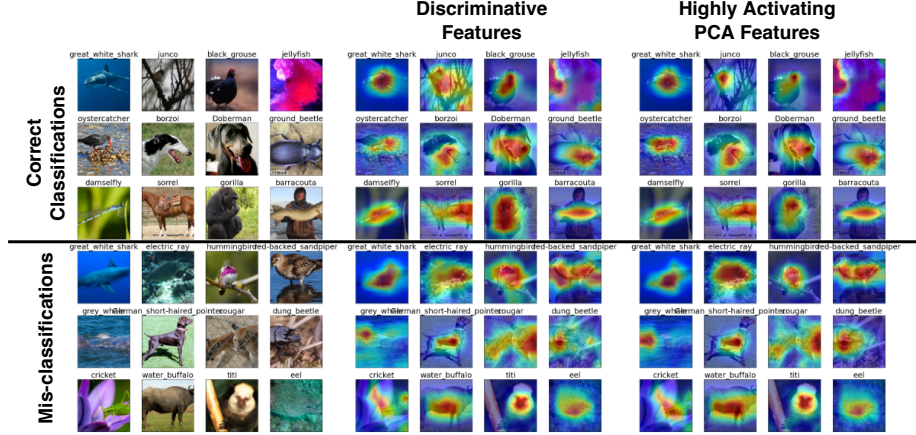


Figure A.3. **Comparing gradient heatmaps of discriminative features and PCA features:** In this figure, we plot the gradient heatmaps of the discriminative features of correct and incorrect classifications on ImageNet-1K trained on SimCLR. We also plot the discriminative PCA features for the same images. We observe that both sets of features activate the same portions of the images meaning that discriminative features can be viewed as axis-aligned.

A.3. Discriminative Features and Principal Components

In our analysis, we select discriminative features independently and observe their heatmaps and activations across the population. Our analysis is based on the assumption that axis-aligned features can provide meaningful information regarding the quality of the feature representations for self-supervised models. To (partially) validate this assumption, we have conducted a PCA analysis where we select principal components of feature representations and perform linear evaluation on top of them. In Figure 3, we observe that, until 40% reduction of the representation size, PCA and (axis-aligned) discriminative features perform comparably in terms of the linear classification accuracy while discriminative features significantly outperforms random features across the board. We also plot the gradients of the highly activating PCA features and compare them to discriminative features in the full representation space in Figure A.3. We observe that both sets of features activate the same portions of the images between both correct and incorrect classifications. These results indicate that axis-aligned discriminative features capture a fair amount of information in the feature representations and thus (partially) validating our underlying assumption.

A.4. Q-Score on Supervised Learning

We note that we select discriminative features and compute Q-Score on self-supervised representations without using any label information. Thus, our study to show correlation between Q-score and classification outcome is non-trivial since self-supervised models learn without labels. Nevertheless, we have included an experiment in Figure A.4, where we analyze Q-score as a predictor of classification outcome (correct vs incorrect) on supervised ResNet-18 (ImageNet-100) and ResNet-50 (ImageNet-1K) representations as well as their robust versions (l2 threat model). Self-supervised representations generally perform better than supervised representations on Q-score indicating that the representational properties we have identified may be mainly prominent in self-supervised learning. We observe that non-robust supervised ResNet shows lower AUROC and AUPRC compared to robust ResNet on both ImageNet-100 and ImageNet-1K setups. This is in line with observations in [22] and [40] that show that robust models provide better axis-alignment of features.

A.5. Transfer Performance of Q-Score Regularization

In Table A.2, we tabulate the transfer learning performance (linear evaluation) of various unseen datasets [34, 35, 17, 36, 37, 7, 33, 16] on 6 self-supervised models trained on ImageNet-1K with and without Q-Score regularization. We use frozen ResNet-50 representations for each transfer dataset (using actual image size) and perform linear evaluation using a classifier. We observe that the average accuracy of unseen datasets improves on all setups, especially on SimCLR, SwaV and MoCo.

In Figure A.5, we visualize the gradient heatmaps of some discriminative features discovered on SimCLR on ImageNet-1K on both ImageNet-1K and unseen datasets, Aircraft [36], Food [7] and Cars [33]. We observe that the physical meaning associated with each feature is consistent between both the training and unseen data. The heatmaps also correspond to informative features, strongly correlated with the ground truth. These gradients indicate that discriminative features are

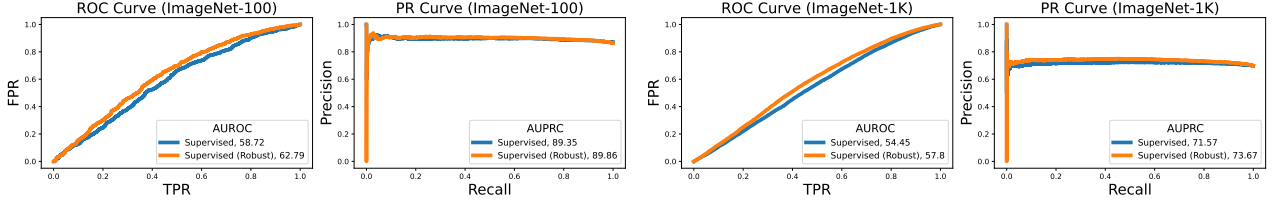


Figure A.4. **Precision-Recall and ROC curves of Q-Score on supervised setups:** In the first two plots, we compute the ROC and PR curves (similar to Figure 5) of Q-score on the representations of a supervised ResNet-18 model and a robust ResNet-18 trained on ImageNet-100. In the last two plots, we show the same for ResNet-50 trained on ImageNet-1K. We observe that robust ResNet performs better for Q-score when used as a predictor for correct or mis-classified representations.

Table A.2. **Transfer learning performance of various state-of-the-art self-supervised models trained on ImageNet-1K with and without Q-Score regularization:** We observe that fine-tuning with Q-Score regularization improves the average transfer accuracy on all self-supervised models.

Transfer Dataset	SimCLR		SwaV		MoCo		BYOL		DINO		SimSiam		VICReg		Barlow Twins	
	Baseline	Q-Score Regularized	Baseline	Q-Score Regularized	Baseline	Q-Score Regularized	Baseline	Q-Score Regularized	Baseline	Q-Score Regularized	Baseline	Q-Score Regularized	Baseline	Q-Score Regularized	Baseline	Q-Score Regularized
CIFAR-10	70.13	70.55	71.27	72.42	72.39	73.26	71.36	72.99	72.62	70.33	72.62	74.29	73.32	73.98	71.23	73.83
CIFAR-100	40.23	40.70	42.52	42.69	45.70	45.70	44.11	45.92	45.36	43.32	46.45	45.85	42.93	42.20	41.01	45.18
STL-10	65.74	65.77	65.81	65.89	66.87	67.03	85.45	86.07	80.07	79.05	71.58	72.76	67.76	74.95	67.38	65.02
Aircraft	62.38	68.13	63.86	73.08	69.34	67.59	63.76	62.14	63.9	73.9	66.5	72.75	68.22	65.69	64.3	63.12
Flowers	88.12	85.19	86.35	86.99	89.19	89.61	87.37	89.59	87.97	89.81	88.54	88.25	85.09	85.69	85.86	87.82
Food	71.68	74.2	77.23	72.82	79.25	79.56	70.69	72.78	71.01	77.87	74.55	71.45	78.03	73.88	72.82	76.82
Cars	51.61	54.26	50.74	53.05	54.37	54.87	51.83	54.85	51.22	51.91	50.92	50.64	52.29	50.44	51.5	53.51
DTD	55.69	56.06	55.63	57.18	55.90	57.12	55.63	56.06	50.9	53.77	52.07	53.24	51.27	52.63	54.07	51.08
Average	63.12	64.36	64.18	65.52	66.62	66.64	66.50	67.48	65.13	67.89	65.33	65.79	64.77	64.91	63.52	64.55



Figure A.5. **Discriminative features on unseen datasets:** We visualize the discriminative features discovered on ImageNet-1K classes on unseen datasets like Aircraft [36], Food [7] and Cars [33]. We observe that discriminative features correspond to the same physical attributes as the training data and are core and informative.

transferable across unseen datasets, which support the improvement we observe in Table A.2.

We also visualize the representations of correct and incorrect classifications of the Flowers [37] dataset in Figure A.6. We use SimCLR pre-trained on ImageNet-1K (top panel) and the same model pre-trained with Q-Score regularization (bottom panel). We observe that the same properties as Figure 4 on ImageNet-1K (train dataset) transfer at test time to Flowers, an unseen dataset. Before regularization, representations, especially the mis-classified ones, do not contain highly activating discriminative features. These features get more enhanced after Q-Score regularization leading to improved top-1 accuracy as shown in Table A.2.

A.6. Q-Score and Classification Confidence

In Figure A.7, we plot the mean of $|L_i|$ (left), i.e., number of highly activating features in the i^{th} sample, and the mean linear classification confidence (right) over the population for each self-supervised model pre-trained with and without Q-Score regularization. We observe an increase in the average number of highly activating features (L_i) and as a result, an improvement in classification confidence, due to more enhanced features.

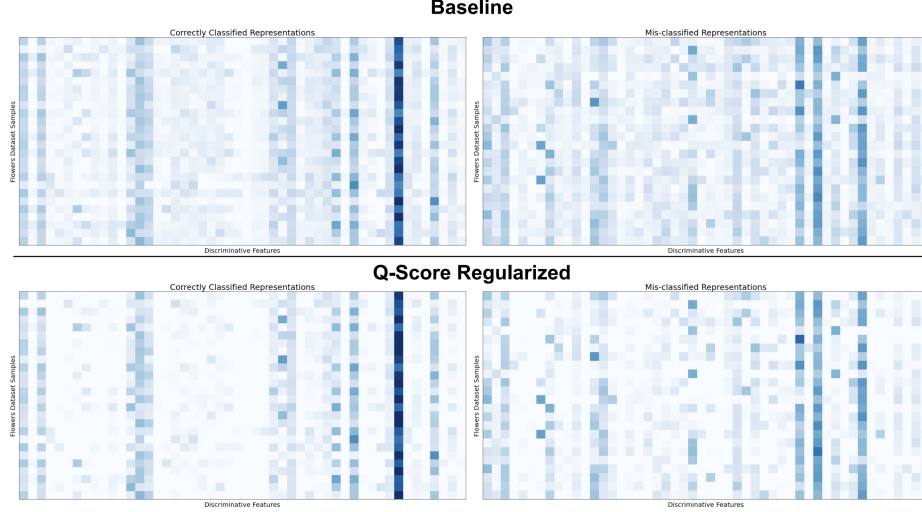


Figure A.6. **Comparing correct and mis-classified representations in Flowers dataset:** In these heatmaps, we visualize the discriminative features of several Flowers [37] dataset samples. In the top panel, we display the correct (left) and incorrect (right) classifications of SimCLR (trained on ImageNet-1K) and in the bottom panel, we visualize the same when pre-trained using Q-Score regularization. Similar to the observations in Figure 4, we observe that the regularization enhances discriminative features, thereby leading to an improvement in performance.

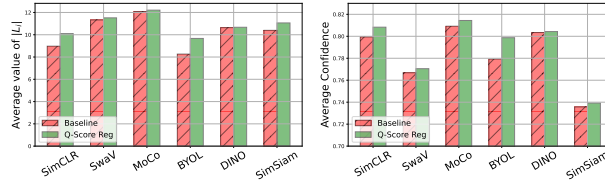


Figure A.7. **Average $|L_i|$ (left) and classification confidence (right) before and after regularization:** On the left we plot the average value of $|L_i|$ (number of highly activating features) and on the right we plot the average classification confidence over the population of ImageNet-1K. We observe that both the number of highly activating features and classification confidence consistently improve on every self-supervised baseline with Q-Score regularization. This improvement is due to the nature of Q-Score regularization which maximizes highly activating discriminative features over the course of pre-training leading to a higher number of such features and improved classification confidence.

A.7. More Gradient Heatmaps of SimCLR

In Figures A.8, A.9, A.10 and A.11, we plot more heatmaps of highly and lowly activating features of SimCLR for 4 different ImageNet-1K classes. We observe that the highly activating features correspond to unique physical properties that are correlated with the ground truth, whereas, lowly activating features, map to spurious portions that do not contribute to useful information.

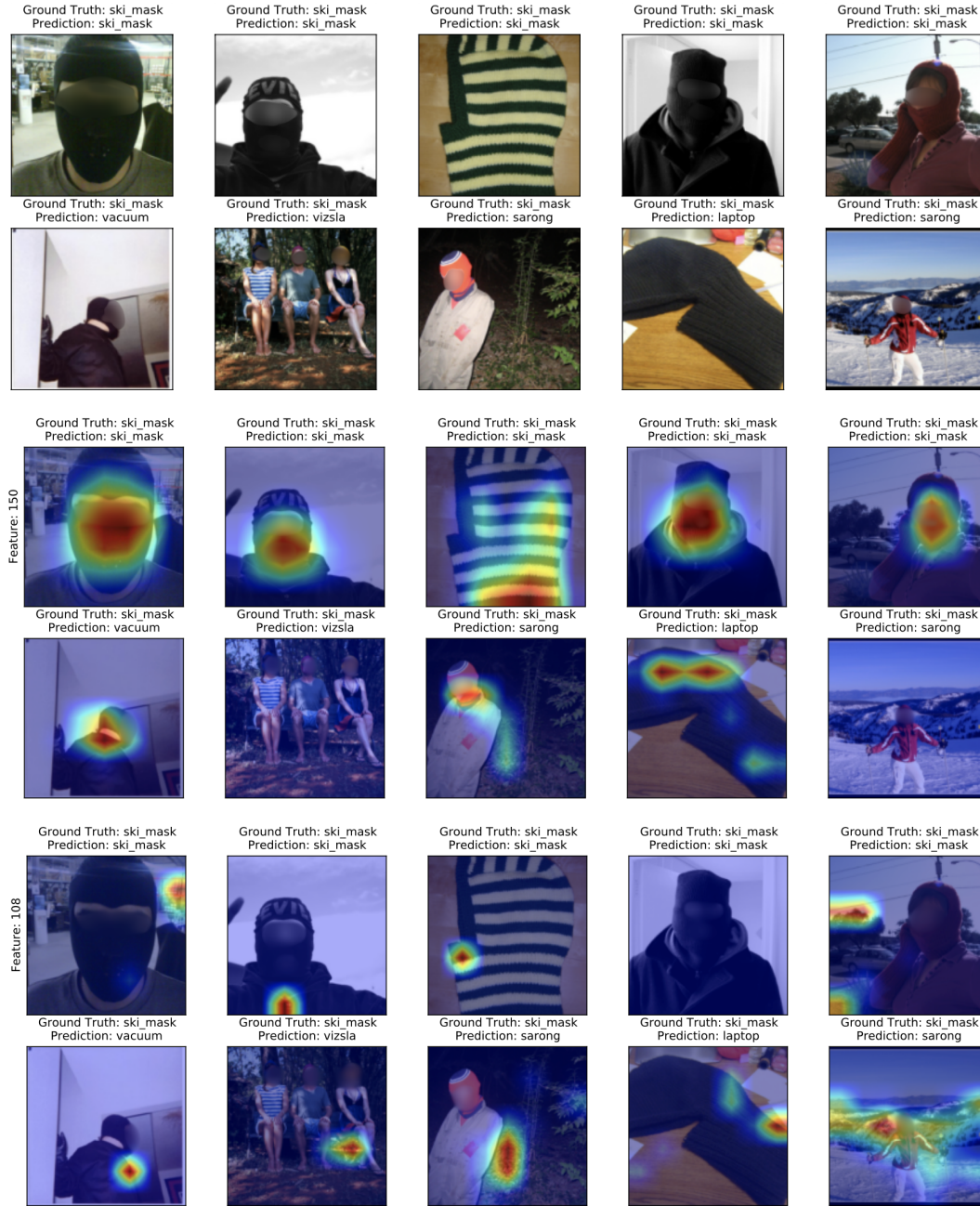


Figure A.8. **Heatmaps of discriminative and lowly activating features of SimCLR (Class - Ski Mask):** We plot the gradient heat maps of the top activating discriminative feature (by magnitude) for the given class and a lowly activating feature of the same class. We observe that discriminative features are more correlated with ground truth labels compared to lowly activating features in both correct and incorrect classification. The discriminative feature in correct classifications correspond to a unique physical attribute that may not exist (or be obfuscated) in mis-classified images.

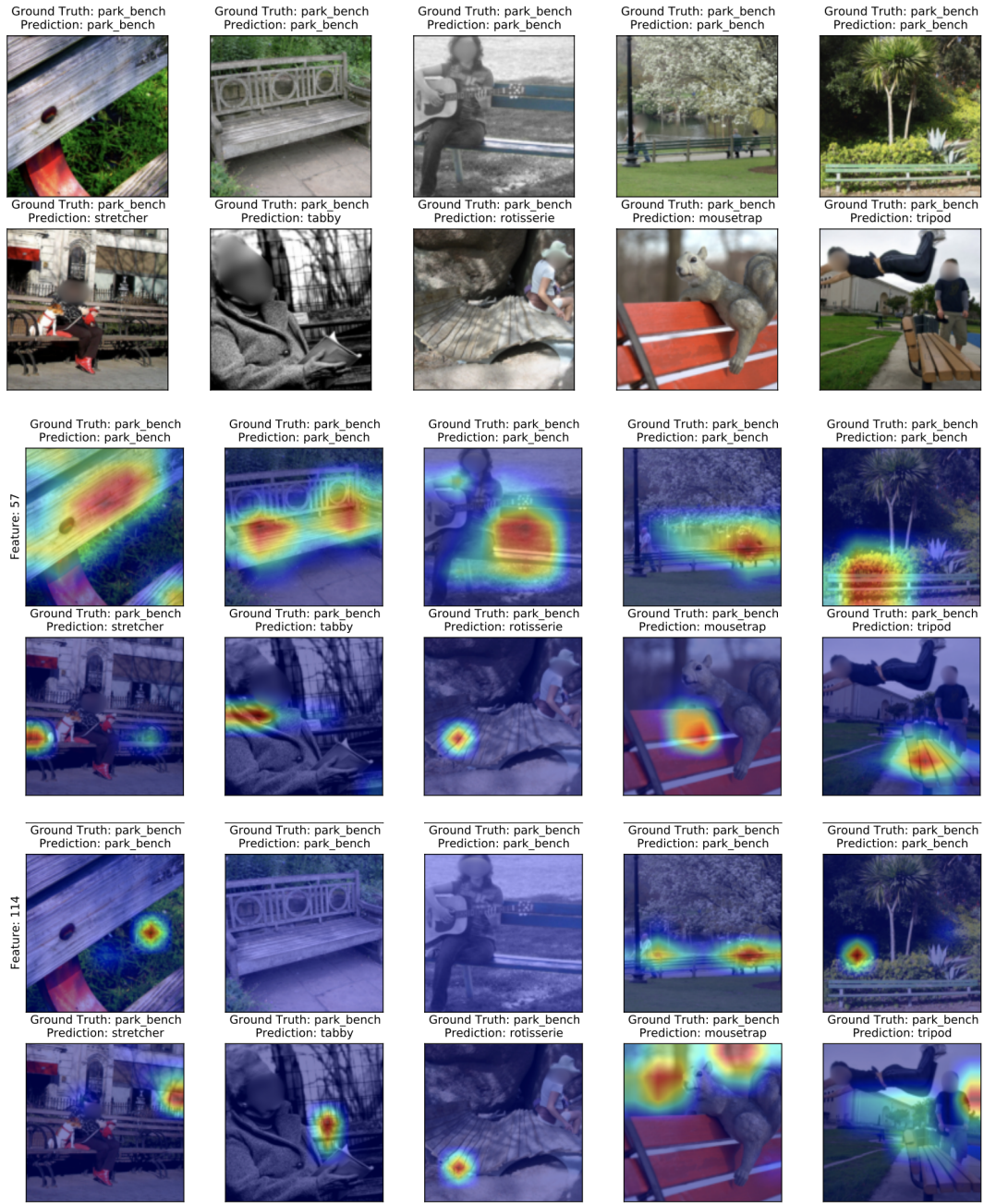


Figure A.9. **Heatmaps of discriminative and lowly activating features of SimCLR (Class - Park Bench):** We plot the gradient heat maps of the top activating discriminative feature (by magnitude) for the given class and a lowly activating feature of the same class. We observe that discriminative features are more correlated with ground truth labels compared to lowly activating features in both correct and incorrect classification. The discriminative feature in correct classifications correspond to a unique physical attribute that may not exist (or be obfuscated) in mis-classified images.

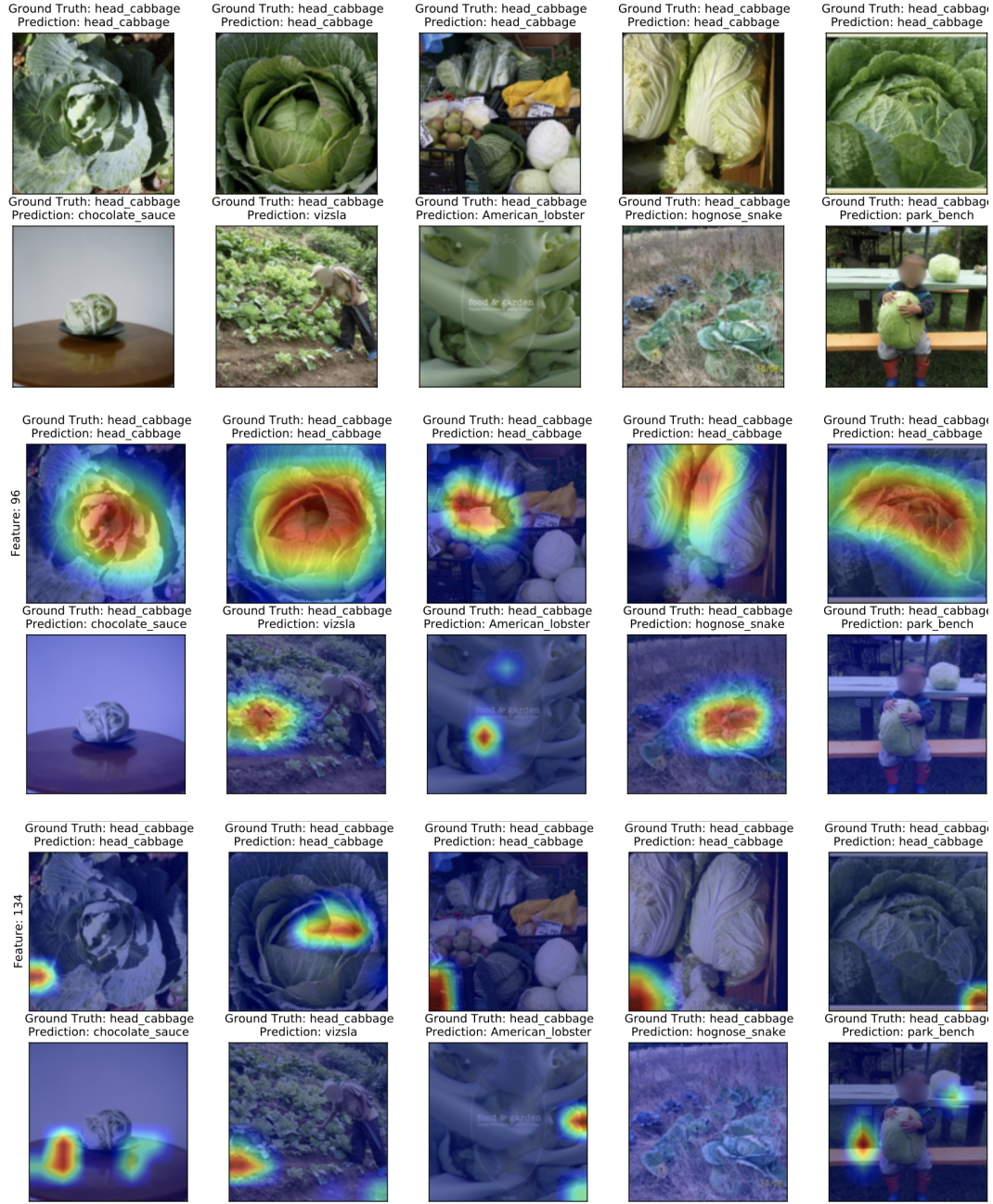


Figure A.10. **Heatmaps of discriminative and lowly activating features of SimCLR (Class - Head Cabbage):** We plot the gradient heat maps of the top activating discriminative feature (by magnitude) for the given class and a lowly activating feature of the same class. We observe that discriminative features are more correlated with ground truth labels compared to lowly activating features in both correct and incorrect classification. The discriminative feature in correct classifications correspond to a unique physical attribute that may not exist (or be obfuscated) in mis-classified images.

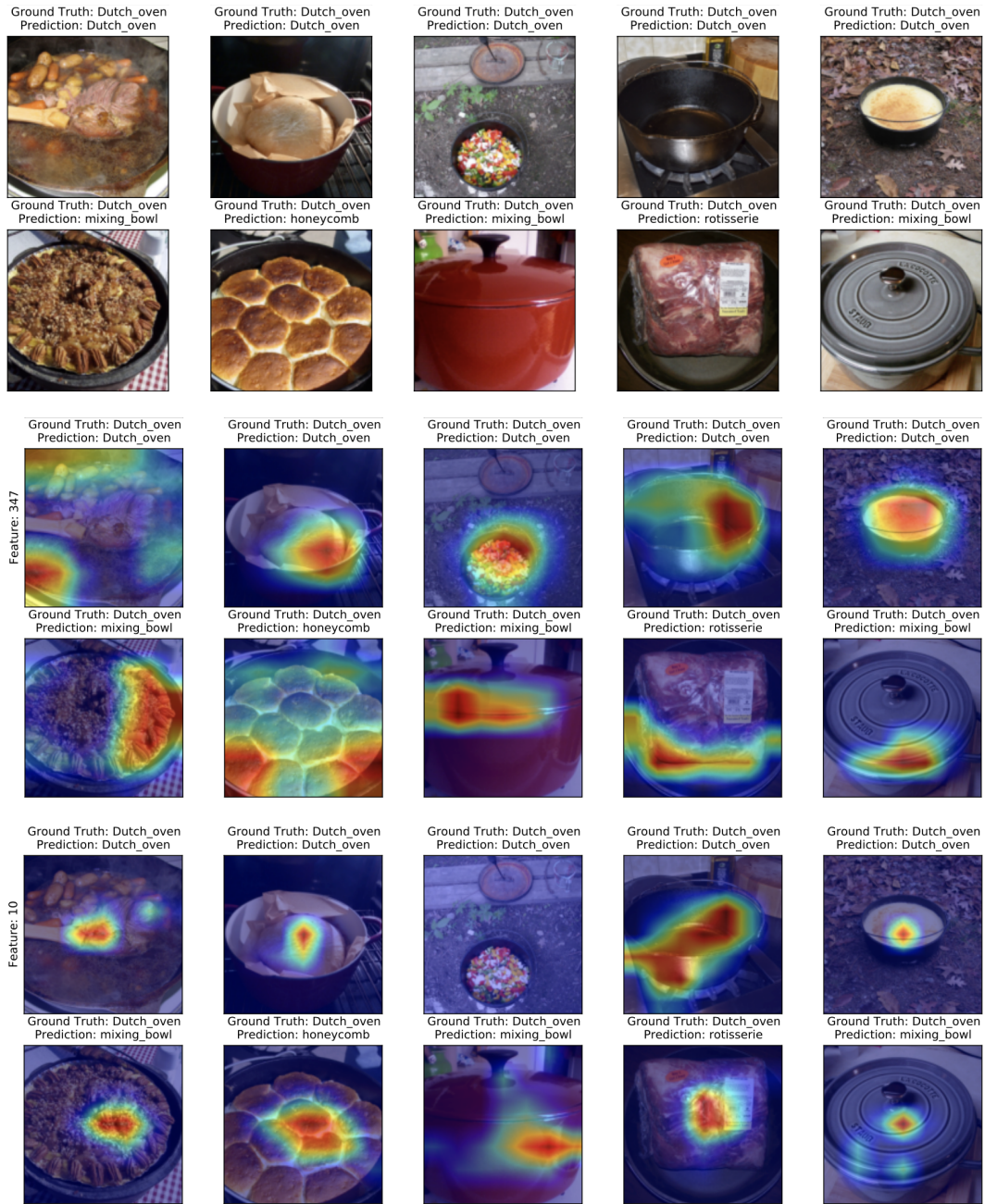


Figure A.11. **Heatmaps of discriminative and lowly activating features of SimCLR (Class - Dutch Oven):** We plot the gradient heat maps of the top activating discriminative feature (by magnitude) for the given class and a lowly activating feature of the same class. We observe that discriminative features are more correlated with ground truth labels compared to lowly activating features in both correct and incorrect classification. The discriminative feature in correct classifications correspond to a unique physical attribute that may not exist (or be obfuscated) in mis-classified images.